Generating Patterns With a Unicycle

Twinkle Tripathy, *Student Member, IEEE*, and Arpita Sinha, *Member, IEEE*

***Abstract*—The objective of the technical note is to make a unicycle trace hypotrochoid like patterns using a simple range based control scheme. These patterns have applications in surveillance, exploration, coverage, etc. In this technical note, the patterns have been characterized in terms of the minimum and maximum radial distance from the center of the pattern. We have shown that under the control scheme and given any controller gain, the agent always achieves a hypotrochoidal pattern. Further, we have shown the existence of controller gains necessary to achieve any desired hypotrochoidal pattern starting from any initial position. We have also analyzed the conditions necessary for the generating patterns in presence of turn rate constraints of the unicycle. The simulations have been performed for the proposed scheme and the mathematical results have been validated.**

***Index Terms*—Autonomous systems, hypotrochoids, pattern generation, range only measurement, unicycle kinematics.**

I. Introduction

The generation of various mathematical patterns has drawn the interest of the research community over several decades as these patterns appear in the nature all around us. For example, growth of a tree, snowflakes, spirals in self organizing dynamic systems, spots and stripes in living beings, paths of astronomical objects, etc., display intricate patterns. These patterns range from very simple lines, triangles, circles and spirals to extremely complex trochoids, cycloids, hypotrochoids, and so on. Many control schemes have been proposed for autonomous vehicles to generate patterns. These control schemes serve engineering applications such as surveillance, exploration, coverage, etc [1].

The development of control laws to generate mathematical patterns has been pursued actively over the past. The literature is rich in control strategies which lead to intricate global formations using single or multiple autonomous agents. When there are multiple agents, it is known as the formation control problem. Advances in the area has been surveyed upon by Cao *et al.* [2]. Several existing works in the literature look at the robots placing themselves into stationary formations of lines, circles or polygons (see [3] and [4]). In certain other works, the agents get into rotationally or translationally invariant dynamic formations resulting in patterns which are rectilinear, polygonal, etc. (refer [5]–[9]). In another approach to formation control problem, along with spatial arrangement of the agents, their trajectories also form patterns, say spirals, epicycles, etc. (see [10]–[13]). Further, there also exists literature which propose strategies to guide robots so that their trajectories follow any pre-specified paths whether independently (single-agent) or cooperatively (multi-agent) (see [14]–[16]).

The work presented in [11]–[13] is more common in spirit with the present work. In [11] and [12], Tsiotras *et al.* have proposed an extension to the standard feedback to address consensus problems for agents with single integrator kinematics. The control law incorporates a term proportional to the direction perpendicular to the relative distance between the agents and their neighbours which is embedded in terms of an error state multiplied with a skew symmetric matrix. This results in improved flexibility on the achievable rendezvous points and the formation of the intricate patterns. The analysis for the patterns is presented for the case of three agents on the plane. In [13], Juang has given the generalization of the cyclic pursuit control scheme, for agents with single integrator kinematics, by the addition of a rotation and a stabilization term. Further, it has been shown by the investigation of the root distribution that one pair of imaginary axis eigen values results in circular formation at steady state whereas two pairs result in epicyclic motions of the agents. Hence, restrictions on the parameters and initial conditions have been elaborated which result in the desired epicyclic formations.

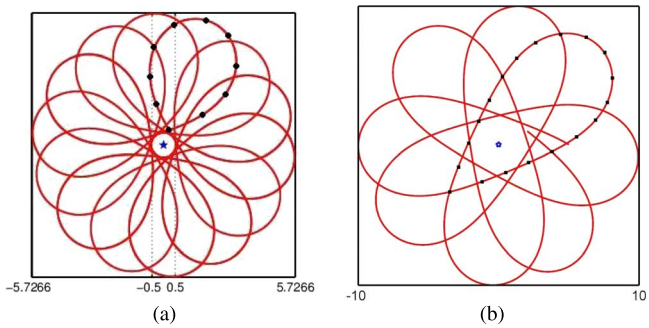

Fig. 1. Patterns generated by unicycle. (a) Type 1. (b) Type 2.

The present work focuses on generating patterns by using only one autonomous agent which is assumed to be unicyclic with a single non-holonomic constraint. The unicycle could represent any autonomous system like aerial vehicle, ground vehicle and so on. Deriving motivation from the work by Tsiotras *et al.* ([11], [12]) and Juang [13], we have proposed a generic control scheme consisting of only a single term which is non-linearly proportional to range (the distance between the agent and the centre point around which the patterns are formed). The preliminary ideas of Section II have been presented in [17] in which a special form of the control scheme has been analyzed. Further results achieved with a specific set of initial conditions have been shown in [18]. Reference [19] discusses the controller gains to achieve desired patterns for the linear form of the control scheme, while the agent is restricted to start from within the annulus only. In this technical note, we have given a more generalized form of the control scheme and the effect of control saturation on the generated patterns.

The proposed control law has been proved to offer the advantage of achieving a hypotrochoid like pattern for every value of the initial condition and the controller gain. The patterns generated by an agent under the proposed scheme are shown in Fig. 1. It can be seen that the patterns are not closed which make them suitable for applications like surveillance and exploration. These patterns have been characterized in terms of the maximum and minimum radial distance from the centre point. It has also been shown that there always exists either a single or a set of values of the controller gain following which the agent can

Manuscript received March 12, 2015; revised July 21, 2015; accepted November 23, 2015. Date of publication November 25, 2015; date of current version September 23, 2016. Recommended by Associate Editor N. Chopra.

The authors are with Systems and Control Engineering, Indian Institute of Technology Bombay, Mumbai 400 076, India (e-mail: twinkle.tripathy@sc.iitb.ac.in; arpita.sinha@iitb.ac.in).

Color versions of one or more of the figures in this paper are available online at http://ieeexplore.ieee.org.

Digital Object Identifier 10.1109/TAC.2015.2503891

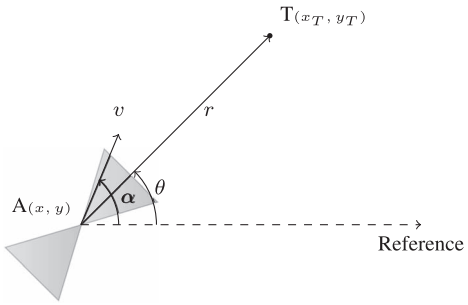

Fig. 2. Engagement geometry between the robot and the target point.

achieve any desired pattern while it can start from any arbitrary initial position and heading direction. A point to be mentioned here is that, the unicycle does not need to know the equation of the hypotrochoid or its tangents at any point. A constant controller gain can achieve the desired pattern. Under constraints on the turn rate, the generation of patterns gets affected as some patterns might demand very high turn rates. The technical note analyzes the effect of turn rate constraints on the pattern generation and gives the necessary conditions to verify whether a pattern can be generated or not or the pattern that can be generated with the given controller parameters. The technical note is organized as follows: In Section II, the patterns are characterized based on the initial conditions and controller gains and in Section III, the conditions on the initial conditions and the controller gain are derived to achieve a hypotrochoid like pattern with desired specifications. The results are verified through simulation in Section IV and Section V concludes the technical note with prospective future work.

II. Analysing the Patterns

This technical note addresses the problem of guiding a mobile robot to trace patterns like hypotrochoid on a plane as shown in Fig. 1. The robot is assumed to have a unicycle model with kinematics

$$\dot{x}(t) = v\cos\alpha(t),\ \dot{y}(t) = v\sin\alpha(t),\ \dot{\alpha}(t) = u(t) \tag{1}$$

where $(x(t), y(t))$ is the position coordinate of the robot at time t,v is the constant linear speed, $\alpha(t)$ is the heading direction and $u(t)$ is the control. Let the pattern be centred at (x_T, y_T) which is defined as the target point T for the robot. With reference to Fig. 2, let r be the line-of-sight (LOS) distance and θ be the LOS angle. Then, the control is designed as

$$u(t) = \eta r^{\mu}(t) \tag{2}$$

where η is the controller gain such that $\eta \neq 0$ is a constant and μ is a positive constant. Denote $\phi = \alpha - \theta$. Then

$$\dot{r} = -v\cos\phi, \quad r\dot{\theta} = -v\sin\phi. \tag{3}$$

Computing $dr/d\phi$ and then rearranging gives $(\eta r^{\mu+1} + v\sin\phi)dr + vr\cos\phi d\phi = 0$. On solving, we get

$$r^{\mu+2} + \frac{(\mu+2)vr\sin\phi}{\eta} = K \tag{4}$$

where K is determined from the initial conditions, $r_0(= r(0))$ and $\phi_0(= \phi(0))$ as

$$K = \left(\frac{(\mu+2)vr_0\sin\phi_0}{\eta} + r_0^{\mu+2}\right). \tag{5}$$

From (3) and (4), $\dot{\theta} = \eta(r^{\mu+2} - K)/((\mu+2)r^2)$. When $K \leq 0$, θ is strictly a monotonic function of time. When $K \geq 0$, similar comments can not be made about θ. However, from (1) and (2), $\dot{\phi} = \dot{\alpha} - \dot{\theta} = (\eta((\mu+1)r^{\mu+2} + K))/((\mu+2)r^2)$, which implies ϕ is strictly monotonic in time. Then, from (3), the sign of $\dot{\theta}$ changes periodically and thus θ is non-monotonic. Fig. 1 shows the patterns for $K \geq 0$ and $K \leq 0$, respectively. A careful observation of the figures shows that the trajectory of the robot forms loops in both the cases. One loop has been manually highlighted with black coloured dots in each of the patterns to differentiate between the type of the loops. For $K \leq 0$, the target point is always inside the loop whereas for $K \geq 0$, it is always outside. This implies that $\dot{\theta}$ is monotonic when $K \leq 0$ and non monotonic otherwise. We define the pattern formed when $K \geq 0$ as *Type 1* pattern [Fig. 1(a)] and when $K \leq 0$ as *Type 2* pattern [Fig. 1(b)]. The applications like boundary surveillance can be served better by *Type 1* patterns. Whereas, for applications where the agent is required to monitor the target point along with the boundary, *Type 2* pattern is more suitable over *Type 1*.

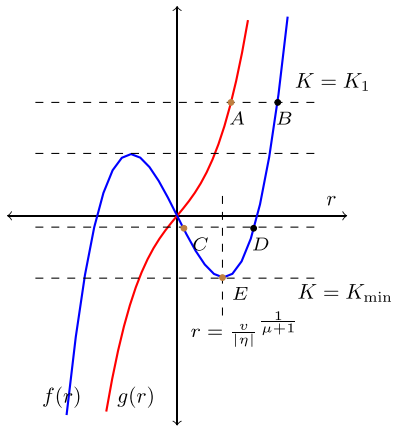

Fig. 3. Solution of (4) for $\phi = \pi/2$ and $\phi = 3\pi/2$.

The hypotrochoidal patterns are bounded in an annulus and, hence, the outer and inner radii of the pattern are denoted by $R_{\max}$ and $R_{\min}$, respectively. Then $r \in [R_{\min}, R_{\max}]$ and we say that the pattern is formed in the region $[R_{\min}, R_{\max}]$.

Lemma 1: $R_{\min}$ occurs when

$$\phi = \begin{cases} \pi/2 & \text{sign}(K) = \text{sign}(\eta) \\ 3\pi/2 & \text{sign}(K) = -\text{sign}(\eta) \end{cases} \tag{6}$$

and $R_{\max}$ occurs when

$$\phi = \begin{cases} 3\pi/2 & \eta > 0 \\ \pi/2 & \eta < 0 \end{cases} \tag{7}$$

independent of the value of K.

Proof: From (3), r attains its maximum and minimum values when $\dot{r} = 0$ which implies $\phi \in \{\pi/2, 3\pi/2\}$ since $\phi \in [0, 2\pi)$. So the following cases are considered:

Case 1: When ($\eta > 0$ and $\phi = 3\pi/2$) or ($\eta < 0$ and $\phi = \pi/2$), the LHS of (4) can be represented as

$$f(r) = r^{\mu+2} - \frac{(\mu+2)vr}{|\eta|} \tag{8}$$

which is a depressed polynomial equation with $f(0) = 0$, $\lim_{r\to\infty} f(r) = \infty$, $f'(0) < 0$ and $f'(r)$ changing sign at $|r| = (v/|\eta|)^{1/(\mu+1)}$. A plot of $f(r)$ is given in Fig. 3. For $f(r) = K$, there is only one sign change in the coefficients of the equation when $K > 0$ and two sign changes when $K \leq 0$. Therefore, from Descartes sign rule [20], there exists one real positive root, say r_f, (point B in

Fig. 3) when $K>0$ and two real positive roots, say $r_{\bar{f}1}$ and $r_{\bar{f}2}$, (points C and D in Fig. 3), when $0 \geq K \geq K_{\min}$. It is evident that if $r_{\bar{f}1} < r_{\bar{f}2}$, then $R_{\max} = r_{\bar{f}2}$ and $R_{\min} = r_{\bar{f}1}$. Using $f'(r)=0$, $K_{\min} = -(\mu+1)(v/|\eta|)^{(\mu+2)/(\mu+1)}$. This is the minimum value K can have for any initial condition. This can also be validated using (5).

Case 2: When ($\eta > 0$ and $\phi = \pi/2$) or ($\eta < 0$ and $\phi = 3\pi/2$), the LHS of (4) can be represented as

$$g(r) = r^{\mu+2} + \frac{(\mu+2)vr}{|\eta|} \tag{9}$$

with $g(0)=0$, $g'(0)>0$ and $\lim_{r\to\infty} g(r) = \infty$, which is plotted in Fig. 3. The coefficients of the equation $g(r)=K$ change sign only once for $K>0$ and do not change sign for $K \leq 0$. Hence, $K>0$ gives only one real positive root, say r_g (point A in Fig. 3) and $K \leq 0$ yields no real positive root.

It is trivial to show that for $K>0$, $r_f > r_g$ and, hence, $R_{\max} = r_f$ and $R_{\min} = r_g$. Therefore, $R_{\max}$ is obtained from (8) irrespective of the value of K and hence, we get (7). Similarly, $R_{\min}$ is obtained from (8) when $K \leq 0$ and from (9) when $K>0$ and hence (6) is satisfied. ■

Remark 1: For any η, v and μ, $K \in [-(\mu+1)(v/|\eta|)^{(\mu+2)/(\mu+1)}, \infty)$. Given an $R_{\max}$, a unique K can be found from (4). However, the same is not true when $R_{\min}$ is given. It is seen from Lemma 1 that if $R_{\min} \in [(v/|\eta|)^{1/(\mu+1)}, \infty)$, only then a unique K is obtained. For $R_{\min} \in [0, (v/|\eta|)^{1/(\mu+1)}]$, always two values of K exist, one positive and one negative, corresponding to Type 1 and Type 2 patterns.

The case when η, v and μ are given, it should be noted that any arbitrary values of $R_{\max}$ and $R_{\min}$ cannot be obtained. We study the range of $R_{\max}$ and $R_{\min}$ for different cases.

Corollary 1: For any initial condition, a robot with kinematics (1) and control (2) generates Type 1 patterns with $R_{\max} \in [((\mu+2)v/|\eta|)^{1/(\mu+1)}, \infty)$ and $R_{\min} \in [0, \infty)$ and Type 2 patterns with $R_{\max} \in [(v/|\eta|)^{1/(\mu+1)}, ((\mu+2)v/|\eta|)^{1/(\mu+1)})$ and $R_{\min} \in [0, (v/|\eta|)^{1/(\mu+1)})$.

Proof: From the proof of Lemma 1, the minimum value of $R_{\max} = (v/|\eta|)^{1/(\mu+1)}$ occurs when $K = K_{\min}$(point E in Fig. 3) and the minimum value of $R_{\min} = 0$ occurs when $K=0$. The maximum value of both go to infinity as $K \to \infty$. When $R_{\max} \in [(v/|\eta|)^{1/(\mu+1)}, ((\mu+2)v/|\eta|)^{1/(\mu+1)}]$, the generated pattern is Type 2 as $K \leq 0$. When $R_{\max} \geq ((\mu+2)v/|\eta|)^{1/(\mu+1)}$, the resulting patterns are Type 1 as $K \geq 0$. ■

Corollary 2: $R_{\max}$ and $R_{\min}$ of a pattern decrease as μ increases, keeping all the other parameters constant.

Proof: From (9), we have $\partial g(r)/\partial r = (\mu+2)(r^{\mu+1} + (v/|\eta|))$ which implies that the slope of $g(r)$ increases as μ increases. Then from the proof of Lemma 1, $R_{\min}$ decreases with increasing μ when $K>0$. Similarly, from (8), $\partial f(r)/\partial r = (\mu+2)(r^{\mu+1} - (v/|\eta|))$ which indicates that its slope increases with μ when $r^{\mu+1} > (v/|\eta|)$ and decreases otherwise. Since, $R_{\max} \in [(v/|\eta|)^{1/(\mu+1)}, \infty)$ from Corollary 1, then $R_{\max}$ decreases with increasing μ. Also, when $K<0$, $R_{\min}$ is evaluated from (8) and $R_{\min} \in [0, (v/|\eta|)^{1/(\mu+1)}]$. Thus, $R_{\min}$ also decreases with increasing μ. ■

Corollary 3: A robot will trace only Type 1 pattern if $r_0 \geq ((\mu+2)v/|\eta|)^{1/(\mu+1)}$.

Proof: For a pattern to be Type 2, K should be negative. This requires $\sin\phi \leq 0$ as rest of terms in (5) are positive. So for any given ϕ_0, we need $K = {r_0}^{\mu+2} - (((\mu+2)v)/\eta){r_0}|\sin\phi_0| \leq 0$. This implies $r_0 \in [0, (((\mu+2)v|\sin\phi_0|)/|\eta|)^{1/(\mu+1)}]$. Using $\sin\phi_0 = -1$, we get the maximum range of r_0. Beyond this maximum value of r_0, K will always be $K>0$ irrespective of the value of ϕ_0 resulting in a Type 1 pattern. ■

When $r_0 \in [0, (((\mu+2)v)/|\eta|)^{1/(\mu+1)}]$, the robot will trace Type 1 pattern if $\sin\phi_0 > -({r_0}^{\mu+1}|\eta|/((\mu+2)v))$ else, it will trace Type 2 pattern. Next, we discuss some interesting cases which arise out of the choice of certain initial conditions and controller parameters.

Corollary 4: When $K = -(\mu+1)(v/|\eta|)^{(\mu+2)/(\mu+1)}$, the pattern generated is a circle of radius $(v/|\eta|)^{1/(\mu+1)}$ centred around the target point.

Proof: $K = -(\mu+1)(v/|\eta|)^{(\mu+2)/(\mu+1)} = K_{\min}$ corresponds to point E in Fig. 3 where $R_{\max} = R_{\min} = (v/|\eta|)^{1/(\mu+1)}$. ■

Corollary 4 corresponds to the condition on K which is necessary to achieve a circle. Further, we show the translation of the condition on K in terms of initial position and heading angle such that the trajectory of the agent is again a circle.

Corollary 5: If $r_0 = (v/|\eta|)^{1/(\mu+1)}$ and if $\phi_0 = 3\pi/2$ when $\eta > 0$ else $\phi_0 = \pi/2$, then the pattern generated is a circle of radius $(v/|\eta|)^{1/(\mu+1)}$.

Proof: From (5), $K = -(\mu+1)(v/|\eta|)^{(\mu+2)/(\mu+1)}$ for the given initial conditions. Hence the proof follows from Corollary 4. ■

If the pattern is required to cover an entire disk of a certain radius, then it becomes mandatory that $R_{\min} = 0$. The obvious solution to the problem is to start at $r_0 = 0$ with any arbitrary heading angle. But sometimes it may not be possible to start such that $r_0 = 0$. So, Corollary 6 covers the conditions to be imposed on any initial conditions to achieve a pattern within a disk.

Corollary 6: If $r_0 = (((\mu+2)v)/|\eta|)^{1/(\mu+1)}$ and if $\phi_0 = 3\pi/2$ when $\eta > 0$ else $\phi_0 = \pi/2$, then the pattern covers a disk of radius $(((\mu+2)v)/|\eta|)^{1/(\mu+1)}$.

Proof: For the given initial conditions, from (4) and (5) $r^{\mu+1} - (((\mu+1)v)/|\eta|)r + (((\mu+1)v/|\eta|){r_0} - {r_0}^{\mu+2}) = 0$. The solution gives $R_{\min} = 0$ and $R_{\max} = ((\mu+2)v/\eta)^{1/(\mu+1)}$ which implies that the entire disk of radius $(((\mu+2)v)/\eta)^{1/(\mu+1)}$ is covered by the pattern. ■

III. Generating the Patterns

This section addresses the problem of how to generate a pattern in a given region when we have the flexibility in the choice of η. The results obtained in this section are crucial from the point of view of applications. For example, when monitoring a landmark it is required for the agent to maintain a certain proximity with the landmark and hence a certain $R_{\min}$. For surveillance, the agent needs to maintain a certain $R_{\max}$ and so on. The first Lemma of the section considers the case when the maximum radius ($R_{\max}$) of the pattern has been specified.

Lemma 2: Given r_0, ϕ_0 and $R_{\max}$ with $R_{\max} \geq r_0$, a robot traces Type 1 pattern if and only if

$$\eta = \begin{cases} \frac{R_{\max} + r_0 \sin\phi_0}{{R_{\max}}^{\mu+2} - {r_0}^{\mu+2}}(\mu+2)v, & \text{when } \sin\phi_0 \geq -\left(\frac{r_0}{R_{\max}}\right)^{\mu+1} \\ \frac{-R_{\max} + r_0 \sin\phi_0}{{R_{\max}}^{\mu+2} - {r_0}^{\mu+2}}(\mu+2)v, & \text{when } \sin\phi_0 \leq \left(\frac{r_0}{R_{\max}}\right)^{\mu+1} \end{cases} \tag{10}$$

and Type 2 pattern if and only if

$$\eta = \begin{cases} \frac{R_{\max} + r_0 \sin\phi_0}{{R_{\max}}^{\mu+2} - {r_0}^{\mu+2}}(\mu+2)v, & \text{when } \sin\phi_0 \leq -\left(\frac{r_0}{R_{\max}}\right)^{\mu+1} \\ \frac{-R_{\max} + r_0 \sin\phi_0}{{R_{\max}}^{\mu+2} - {r_0}^{\mu+2}}(\mu+2)v, & \text{when } \sin\phi_0 \geq \left(\frac{r_0}{R_{\max}}\right)^{\mu+1} \end{cases}. \tag{11}$$

Proof: When r_0, ϕ_0 and $R_{\max}$ are given, from (4), (5), and Lemma 1, $K = R_{max}^{\mu+2} - ((\mu+2)v R_{\max})/|\eta| = {r_0}^{\mu+2} + ((\mu+2)v{r_0}\sin\phi_0)/|\eta|$ from which we get two values of η as $\eta_1 = ((R_{\max} + r_0\sin\phi_0)/({R_{\max}}^{\mu+2} - {r_0}^{\mu+2}))(\mu+2)v$ and $\eta_2 = (-R_{\max} + r_0\sin\phi_0)/({R_{\max}}^{\mu+2} - {r_0}^{\mu+2}))(\mu+2)v$ and the corresponding K as $K_1 = R_{\max}{r_0}\ (({R_{\max}}^{\mu+1}\sin\phi_0 + {r_0}^{\mu+1})/(R_{\max} + r_0\sin\phi_0))$ and $K_2 = R_{\max}{r_0}\ (({R_{\max}}^{\mu+1}\sin\phi_0 - {r_0}^{\mu+1})/(-R_{\max} + r_0\sin\phi_0))$. It can be verified that $\eta_1 > 0$, $\eta_2 < 0$, $K_1 \geq 0$ when $\sin\phi_0 \geq -(r_0/R_{\max})^{\mu+1}$ and $K_2 \geq 0$ when $\sin\phi_0 \leq (r_0/R_{\max})^{\mu+1}$. Therefore, the necessary condition to get Type 1 pattern is that $K \geq 0$ which will be

true if η satisfies (10). Similarly, for Type 2 pattern $K \leq 0$ which is achieved when η satisfies (11). To prove the sufficiency condition, we need to show that in order to get *Type 1* pattern, that is, $K \geq 0$, η is as given in (10) and otherwise it is as given in (11). This is also true from the preceding argument. ■

The corresponding value of $R_{\min}$ for Lemma 2 can be calculated as the root of either (8) or (9) depending on the value of K. Next, when $R_{\min}$ is specified beyond which the pattern should be formed, the result is stated in the following Lemma. The proof is similar to Lemma 2 and so is omitted.

Lemma 3: Given r_0, ϕ_0 and $R_{\min}$ with $R_{\min} \leq r_0$, a robot traces Type 1 pattern if and only if

$$\eta = \begin{cases} \frac{R_{\min}+r_0 \sin\phi_0}{{R_{\min}}^{\mu+2}-{r_0}^{\mu+2}}(\mu+2)v, & \text{when } \sin\phi_0 \geq -\frac{R_{\min}}{r_0} \\ \frac{-R_{\min}+r_0 \sin\phi_0}{{R_{\min}}^{\mu+2}-{r_0}^{\mu+2}}(\mu+2)v, & \text{when } \sin\phi_0 \leq \frac{R_{\min}}{r_0} \end{cases} \quad (12)$$

and Type 2 pattern if and only if

$$\eta = \begin{cases} \frac{R_{\min}+r_0 \sin\phi_0}{{R_{\min}}^{\mu+2}-{r_0}^{\mu+2}}(\mu+2)v, & \text{when } \sin\phi_0 \leq -\frac{R_{\min}}{r_0} \\ \frac{-R_{\min}+r_0 \sin\phi_0}{{R_{\min}}^{\mu+2}-{r_0}^{\mu+2}}(\mu+2)v, & \text{when } \sin\phi_0 \geq \frac{R_{\min}}{r_0}. \end{cases} \quad (13)$$

The corresponding value of $R_{\max}$ for Lemma 3 is given by the solution of (8) using the value of K obtained in Lemma 3.

Remark 2: From Lemma 2 and 3, we observe that *Type 2* pattern will not exist if $-(R_{\min}/r_0) \leq \sin\phi_0 \leq (R_{\min}/r_0)$ or $-(r_0/R_{\max})^{\mu+1} \leq \sin\phi_0 \leq (r_0/R_{\max})^{\mu+1}$. This is pictorially represented in Fig. 2 as the shaded region. If the heading is inside the shaded region, *Type 2* patterns are infeasible. Such restrictions do not exist for *Type 1* patterns. We have not analyzed the cause for such restrictions, since we have technical note limitation and our main aim is to design the controller in the most general situation.

Next, we consider both $R_{\max}$ and $R_{\min}$ are given.

Corollary 7: A robot traces a pattern in the region $[R_{\min}, R_{\max}]$, if and only if

$$\eta = \pm\frac{R_{\max} \pm R_{\min}}{R_{\max}^{\mu+2} - R_{\min}^{\mu+2}}(\mu+2)v. \quad (14)$$

Proof: The proof follows from (4) and Lemma 1 and is in the line of Lemma 2 and 3. Hence, the details are omitted. ■

There are four possible values of η in (14). From (4), we have

$$K = \begin{cases} \frac{R_{\max}R_{\min}\left(R_{\max}^{\mu+1}+R_{\min}^{\mu+1}\right)}{R_{\max}+R_{\min}} \geq 0 & \eta = \pm\frac{R_{\max}+R_{\min}}{R_{\max}^{\mu+2}-R_{\min}^{\mu+2}}(\mu+2)v \\ \frac{R_{\max}R_{\min}\left(-R_{\max}^{\mu+1}+R_{\min}^{\mu+1}\right)}{R_{\max}-R_{\min}} \leq 0 & \eta = \pm\frac{R_{\max}-R_{\min}}{R_{\max}^{\mu+2}-R_{\min}^{\mu+2}}(\mu+2)v. \end{cases} \quad (15)$$

Hence, two of the controller gains result in *Type 1* patterns and two others result in *Type 2* patterns. Corollary 7 does not consider the initial conditions in calculating the controller gain. However, any initial condition does not result in covering the desired region since (4) and (5) may not be satisfied simultaneously. We will address this later in the technical note. Next, we find the relation between $R_{\max}$, $R_{\min}$ and instantaneous r and ϕ.

Lemma 4: Given $R_{\max}$, $R_{\min}$ and any arbitrary instantaneous r, a robot traces a Type 1 pattern if and only if

$$\sin\phi = \pm\frac{R_{\max}\left(R_{\min}^{\mu+2} - r^{\mu+2}\right) + R_{\min}\left(R_{\max}^{\mu+2} - r^{\mu+2}\right)}{r\left(R_{\max}^{\mu+2} - R_{\min}^{\mu+2}\right)} \quad (16)$$

and a Type 2 pattern if and only if

$$\sin\phi = \pm\frac{R_{\max}\left(R_{\min}^{\mu+2} - r^{\mu+2}\right) - R_{\min}\left(R_{\max}^{\mu+2} - r^{\mu+2}\right)}{r\left(R_{\max}^{\mu+2} - R_{\min}^{\mu+2}\right)}. \quad (17)$$

Proof: From Corollary 7, we get the possible η values and the corresponding K is given in (15). The necessary condition is obtained by applying (15) in (4) to find the values of instantaneous ϕ given by (16) and (17). The sufficiency condition is obtained by using the values of ϕ from (16) and (17) in (4) and then calculating K to find its sign. ■

For a given $R_{\max}$, $R_{\min}$, and r, there are four possible values of $\sin\phi$ and each one corresponds to one of the η in (14). Therefore, there are eight possible values of ϕ.

Corollary 8: A robot traces a pattern in $[R_{\min}, R_{\max}]$ if $r_0 \in [R_{\min}, R_{\max}]$.

Proof: In Lemma 4, ϕ will exist if and only if the right hand side of (16) and (17) are bounded within ± 1. Let us denote $\Phi_1 = (R_{\max}(R_{\min}^{\mu+2} - r^{\mu+2}) + R_{\min}(R_{\max}^{\mu+2} - r^{\mu+2}))/(r(R_{\max}^{\mu+2} - R_{\min}^{\mu+2}))$ and $\Phi_2 = (R_{\max}(R_{\min}^{\mu+2} - r^{\mu+2}) - R_{\min}(R_{\max}^{\mu+2} - r^{\mu+2}))/(r(R_{\max}^{\mu+2} - R_{\min}^{\mu+2}))$. For $\Phi_1 \geq -1$, we get $(R_{\max} - r_0)(\sum_{l=0}^{l=m+1} {r_0}^l({R_{\max}}{R_{\min}}^{\mu+1-l} + {R_{\min}}^{\mu+2-l} + r_0({R_{\max}}^{\mu+1-l} - {R_{\min}}^{\mu+1-l}))) \geq 0$ which will hold if $R_{\max} \geq r_0$ since the terms inside the summation are always positive. For $\Phi_1 \leq 1$, $(R_{\min} - r_0)((R_{\max} - r_0)\sum_{l=0}^{l=m+1} {r_0}^l {R_{\max}}^{\mu+1-l} + (R_{\max} + r_0)\sum_{l=0}^{l=m+1} {r_0}^l {R_{\min}}^{\mu+1-l}) \leq 0$ which will hold if $R_{\min} \leq r_0$ because $R_{\max} \geq r_0$ (as shown in the previous condition) and the other terms are all positive. Therefore, from (16), we must have $r_0 \in [R_{\min}, R_{\max}]$. Similarly, for $\Phi_2 \geq 1$, we get $(R_{\max - r_0})(R_{\min} - r_0)\sum_{l=0}^{l=m+1}(R_{\max}^l - R_{\min}^l){r_0}^{\mu+1-l} \leq 0$ and can be satisfied only when $r_0 \in [R_{\min}, R_{\max}]$. ■

Remark 3: The sufficiency of Corollary 8 requires conditions on ϕ_0 which are presented in Lemma 4.

Any arbitrarily chosen values of $R_{\max}$, $R_{\min}$, r_0, and ϕ_0 will not necessarily satisfy Lemma 4 which implies that there does not exist a η to form the pattern. However, we can circumvent this situation by using two values of η and switching at an appropriate instant. This is discussed in the following theorem.

Theorem 1: Given r_0, ϕ_0, $R_{\min}$, and $R_{\max}$, a robot can trace a pattern in $[R_{\min}, R_{\max}]$ if the controller gain is switched at any instantaneous $r \in [R_{\min}, R_{\max}]$ from η_i to η_f, where η_i and η_f take one of the four possible values

$$\eta_{i1} = (\mu+2)v\left\{\frac{{R_{\max}}^{\mu+2}(r_0\sin\phi_0 - R_{\min})}{(r^{\mu+2} - {r_0}^{\mu+2})\left({R_{\max}}^{\mu+2} - {R_{\min}}^{\mu+2}\right)} + \frac{-{R_{\min}}^{\mu+2}(r_0\sin\phi_0 + R_{\max}) + r^{\mu+2}(R_{\max}+R_{\min})}{(r^{\mu+2} - {r_0}^{\mu+2})\left({R_{\max}}^{\mu+2} - {R_{\min}}^{\mu+2}\right)}\right\}$$

$$\eta_{f1} = (\mu+2)v\frac{R_{\max}+R_{\min}}{{R_{\max}}^{\mu+2} - {R_{\min}}^{\mu+2}} \quad (18)$$

$$\eta_{i2} = (\mu+2)v\left\{\frac{{R_{\max}}^{\mu+2}(r_0\sin\phi_0 + R_{\min})}{(r^{\mu+2} - {r_0}^{\mu+2})\left({R_{\max}}^{\mu+2} - {R_{\min}}^{\mu+2}\right)} + \frac{-{R_{\min}}^{\mu+2}(r_0\sin\phi_0 + R_{\max}) + r^{\mu+2}(R_{\max}-R_{\min})}{(r^{\mu+2} - {r_0}^{\mu+2})\left({R_{\max}}^{\mu+2} - {R_{\min}}^{\mu+2}\right)}\right\}$$

$$\eta_{f2} = (\mu+2)v\frac{R_{\max}-R_{\min}}{{R_{\max}}^{\mu+2} - {R_{\min}}^{\mu+2}} \quad (19)$$

$$\eta_{i3} = (\mu+2)v\left\{\frac{{R_{\max}}^{\mu+2}(r_0\sin\phi_0 + R_{\min})}{(r^{\mu+2} - {r_0}^{\mu+2})\left({R_{\max}}^{\mu+2} - {R_{\min}}^{\mu+2}\right)} - \frac{{R_{\min}}^{\mu+2}(r_0\sin\phi_0 - R_{\max}) + r^{\mu+2}(R_{\max}+R_{\min})}{(r^{\mu+2} - {r_0}^{\mu+2})\left({R_{\max}}^{\mu+2} - {R_{\min}}^{\mu+2}\right)}\right\}$$

$$\eta_{f3} = -(\mu+2)v\frac{R_{\max}+R_{\min}}{{R_{\max}}^{\mu+2} - {R_{\min}}^{\mu+2}} \quad (20)$$

$$\eta_{i4} = (\mu+2)v\left\{\frac{{R_{\max}}^{\mu+2}(r_0\sin\phi_0 - R_{\min})}{(r^{\mu+2} - {r_0}^{\mu+2})\left({R_{\max}}^{\mu+2} - {R_{\min}}^{\mu+2}\right)} - \frac{{R_{\min}}^{\mu+2}(r_0\sin\phi_0 - R_{\max}) + r^{\mu+2}(R_{\max}-R_{\min})}{(r^{\mu+2} - {r_0}^{\mu+2})\left({R_{\max}}^{\mu+2} - {R_{\min}}^{\mu+2}\right)}\right\}$$

$$\eta_{f4} = -(\mu+2)v\frac{R_{\max}-R_{\min}}{{R_{\max}}^{\mu+2} - {R_{\min}}^{\mu+2}}. \quad (21)$$

TABLE I
SIMULATION RESULTS

	r_0	ϕ_0	μ	η	K	$R_{\max}$		$R_{\min}$		ω_1	ω_2	$\dot{\alpha}_{\max}$
						Analytical	Simulation	Analytical	Simulation			
Case 1	1	150	1	0.5	16	5.73	5.73	0.53	0.53	1.58	2.74	2.86
Case 2	5	330	2	0.016	-2500	10.00	10.00	2.01	2.01	0.74	1.86	1.6
Case 3	10	45	1	-0.4632	771	10.34	10.34	8.00	8.00	1.52	2.64	4.79
Case 4	20	-3.4	1	0.01178	6485	38.00	38.00	5.00	5.00	0.24	0.42	0.45
Case 5	30	45	1	$\eta_i = -0.01096$, $\eta_f = 0.0476$	1700	20	20.04	5	5.08	0.49	0.84	0.95
	2	45	1	$\eta_i = 0.0127$, $\eta_f = 0.02900$	2708	25	24.92	5	4.82	0.38	0.66	0.72
Case 6	1	150	2	0.05	201	7.53	7.53	0.5023	0.5023	1.08	2.71	2.84
	1	150	3	0.05	251	4.85	4.85	0.5019	0.5019	1.58	5.29	5.70
	1	150	5	0.05	351	3.06	3.06	0.5014	0.5014	2.32	11.75	13.19
	1	150	10	0.05	601	1.95	1.95	0.5006	0.5006	3.29	31.49	37.76

Proof: Given $R_{\max}$ and $R_{\min}$, from Corollary 7, we get four possible values of η_f and from Lemma 4, we get four possible values of $\sin\phi$ for any $r \in [R_{\min}, R_{\min}]$. There is a one-to-one correspondence between each value of η_f and $\sin\phi$ obtained from Corollary 7 and Lemma 4 respectively. Now, for each $\sin\phi$, we can find η from (4) and (5) since r_0, ϕ_0 and r are known and it will correspond to η_i. These are given in (18)–(21). ■

Theorem 1 allows the robot to start from anywhere in the plane with any arbitrary heading direction and achieve the hypotrochoidal pattern in the given region $[R_{\min}, R_{\max}]$. The pattern will be of Type 1 if (18) or (20) is selected, else it will be of Type 2. If r_0, ϕ_0, $R_{\max}$ and $R_{\min}$ satisfy (4) and (5) simultaneously, then $\eta_i = \eta_f$. In this work, we emphasise on designing the control law to generate the desired pattern. It does not use any feedback to ensure that there is no error in the desired and actual pattern generated.

In some applications, there are constraints on the maximum turn rate of an agent. Such constraints give bounds on the maximum control input. We analyze the effect of input bounds on the generation of patterns ($R_{\max}$ and $R_{\min}$) for any η and μ. Let the maximum turn rate a robot can have be $\omega_{\max} \geq 0$. Then, we should have $|u| = |\eta r^{\mu}| \leq \omega_{\max}$, $\forall\, t > 0$. Since $r \in [R_{\min}, R_{\max}]$, the turn rate constraint will always be satisfied if

$$|\eta R_{\max}^{\mu}| \leq \omega_{\max}. \tag{22}$$

For given η and μ, as we vary ϕ_0 and r_0, we get different $R_{\max}$ and $R_{\min}$. When there is a constraint on $\omega_{\max}$, the achievable values of $R_{\max}$ and $R_{\min}$ get narrowed as discussed below.

Theorem 2: Given η and μ, the robot will trace:

1) no pattern if $\omega_{\max} < \omega_1$;
2) only Type 2 pattern if $\omega_1 \leq \omega_{\max} \leq \omega_2$
3) both Type 1 and 2 pattern if $\omega_{\max} \geq \omega_2$

where

$$\omega_1 = v^{\frac{\mu}{(\mu+1)}} |\eta|^{\frac{1}{(\mu+1)}},\ \omega_2 = ((\mu+2)v)^{\frac{\mu}{(\mu+1)}} |\eta|^{\frac{1}{(\mu+1)}}. \tag{23}$$

Proof: From (22), let the upper bound of $R_{\max}$ be denoted by $\bar{R}_{\max} = (\omega_{\max}/|\eta|)^{1/\mu}$. From Corollary 1, if $\bar{R}_{\max} < (v/|\eta|)^{1/(\mu+1)}$, which implies $\omega_{\max} \leq \omega_1$ then, neither Type 1 nor Type 2 patterns are possible. Similarly, if $(v/|\eta|)^{1/(\mu+1)} \leq \bar{R}_{\max} \leq (((\mu+2)v)/|\eta|)^{1/(\mu+1)}$, then only Type 2 patterns are possible and if $\bar{R}_{\max} > (((\mu+2)v)/|\eta|)^{1/(\mu+1)}$, then both the patterns are possible. ■

Remark 4: When $(v/|\eta|)^{1/(\mu+1)} \leq \bar{R}_{\max} \leq (((\mu+2)v)/|\eta|)^{1/(\mu+1)}$, $R_{\max} \in [(v/|\eta|)^{1/(\mu+1)}, \bar{R}_{\max}]$. Corresponding bounds on $R_{\min}$ can be obtained from (4) by solving $R_{\min}^{\mu+2} - ((\mu+2)vR_{\min})/|\eta| = (\omega_{\max}/|\eta|)^{(\mu+2)/\mu} - ((\mu+2)v(\omega_{\max})^{1/\mu}/|\eta|^{(\mu+1)/\mu})$. Let us denote it as $\bar{R}_{\min}$. Then, $R_{\min} \in [(v/|\eta|)^{1/(\mu+1)}, \bar{R}_{\min}]$. When $\bar{R}_{\max} \geq (((\mu+2)v)/|\eta|)^{1/(\mu+1)}$, the bounds on $R_{\max}$ and $R_{\min}$ are the same as stated in Corollary 1 for Type 2 patterns. However, for Type 1 pattern, $R_{\max} \in [(((\mu+2)v)/|\eta|)^{1/(\mu+1)}, \bar{R}_{\max}]$ and $R_{\min} \in [0, \bar{R}'_{\min}]$ where $\bar{R}'_{\min}$ can be obtained from (4) by solving $R_{\min}^{\mu+2} + ((\mu+2)vR_{\min}/|\eta|) = (\omega_{\max}/|\eta|)^{(\mu+2)/\mu} - ((\mu+2)v(\omega_{\max})^{1/\mu}/|\eta|^{(\mu+1)/\mu})$.

IV. SIMULATION RESULTS

We simulate different scenarios with the initial conditions and the parameters used in simulation as given in Table I. In all the cases, we assumed that $v = 5$ units and μ as given in the table.

Case 1: We assume that r_0 and ϕ_0 are given. For $\eta = 0.05$, from (4), $K = 151$ implying a Type 1 pattern. The trajectory of the robot is plotted in Fig. 1(a). The values of $R_{\max}$ and $R_{\min}$ calculated using Lemma 1 with (4) and observed in simulation match exactly (refer to Table I).

Case 2: We assume that r_0, ϕ_0 and $R_{\max}$ are given. Then $\sin\phi_0 \leq -(r_0/R_{\max})^{\mu+1}$ and from Lemma 2, $\eta_1 = -0.00133$ and $\eta_2 = 0.016$. According to lemma, η_2 will generate Type 2 pattern which can be verified from the trajectory plotted in Fig. 1(b).

Case 3: We assume that r_0, ϕ_0 and $R_{\min}$ are given. Then $\sin\phi_0 < (R_{\min}/r_0)$ and the possible η values are -0.4632 and 0.0019. From Lemma 3, $\eta = -0.4632$ gives $K = 771.039$ and, hence, Type 1 pattern which is validated in Fig. 4(a).

Case 4: We assume that $R_{\max}$ and $R_{\min}$ have been specified. From Corollary 7, we get $\eta = \pm 0.01178$ and $\eta = \pm 0.00904$. The initial conditions are given by Lemma 4 and Corollary 8. So, $r_0 = 20$ and $\phi_0 = -3.3976$ are chosen. For $\eta = 0.01178$, $K = 6484.90$ resulting in a Type 1 pattern as shown in Fig. 4(b). The $R_{\max}$ and $R_{\min}$ achieved through simulation verify the theoretical results as shown in Table I.

Case 5: Here, $R_{\max}$ and $R_{\min}$ are given with $r_0 \notin [R_{\min}, R_{\max}]$. We have considered two cases. In the first case, $r_0 \geq R_{\max}$. Theorem 1 implies that switching of η is required at any arbitrary $r \in [R_{\min}, R_{\max}]$. Let $r = 15.2$, then the trajectory with one of the possible set of controller gains given in Table I is shown in Fig. 4(c) with the initial and final desired patterns being given in different colours. In the second case, $r_0 \leq R_{\max}$. In this case, we switch at $r = 10$, the trajectory of the agent is shown in Fig. 4(d)

Case 6: Here, we vary μ keeping all the other parameters and initial conditions same. The trajectories of the robot are shown in Fig. 5. In accordance to Corollary 2, the $R_{\max}$ and $R_{\min}$ decrease with increase in μ. It is also tabulated in Table I.

In all the cases above, we have calculated ω_1 and ω_2 from (23) and also noted the maximum turn rate of the robot in Table I. For all Type 2 patterns (that is, Case 2), $\omega_1 \leq \dot{\alpha}_{\max} \leq \omega_2$ and for all Type 1 patterns (that is, all the cases except Case 2), $\dot{\alpha}_{\max} \geq \omega_2$. This shows that if we have a turn rate constraint, $\omega_{\max}$ which satisfies $\dot{\alpha}_{\max} \leq \omega_{\max}$, then $\omega_{\max}$ must satisfy the conditions given in Theorem 2.

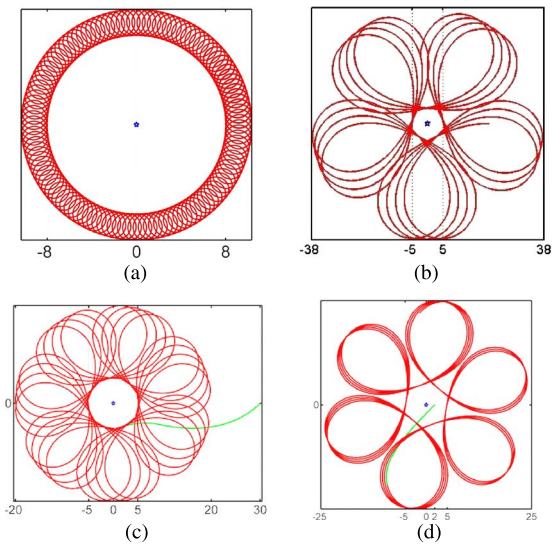

Fig. 4. Trajectory of the robot for different cases. (a) Case 3. (b) Case 4. (c) Case 5: $r_0 > R_{\max}$. (d) Case 5: $r_0 < R_{\min}$.

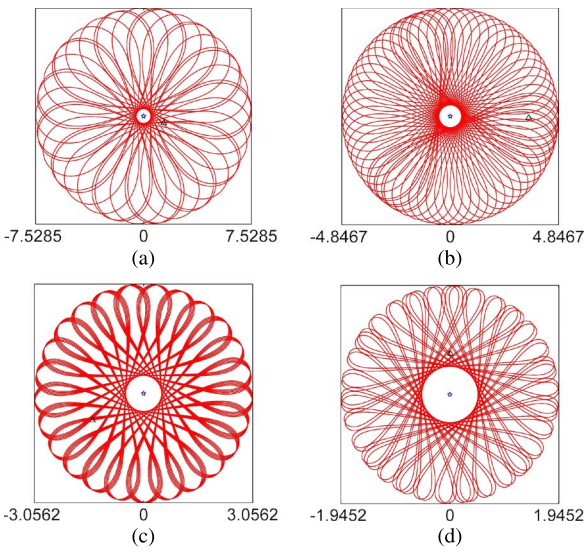

Fig. 5. Effect of μ. (a) $\mu = 2$. (b) $\mu = 3$. (c) $\mu = 5$. (d) $\mu = 10$.

V. Conclusion

Mathematical patterns appear abundantly in nature and have always drawn the interest of the research community. In this technical note, we have proposed a simple non-linear control scheme that renders intricate hypotrochoidal patterns in a plane. The scheme uses a single agent, modelled as a unicycle. The control input to the agent is non-linearly proportional to the radial distance of the agent from the centre of the pattern. Under the control scheme, it has been shown that given any controller gain and starting from any initial position, the agent achieves a hypotrochoid like pattern. Also, we have shown the conditions on the agent's position and the controller gain necessary to achieve a desired pattern which has been specified in terms of either the minimum radial distance from the pattern's centre or the maximum radial distance or both. Further, we have provided the necessary restrictions on the possible patterns that can be generated by the proposed control law in the presence of turn rate constraints on the unicycle. As an extension to this work, further analysis can be done to mathematically characterise the hypotrochoidal parameters in terms of the controller parameters and the initial coordinates of the agent. Also, we can look into the time stamping of the pattern, that is, finding the time required to complete certain percentage of the pattern.

References

[1] P. H. Batavia, S. A. Roth, and S. Singh, "Autonomous coverage operations in semi-structured outdoor environments," in *Proc. IEEW/RSJ Int. Conf. Intelligent Robots and Systems*, 2002, pp. 743–749.

[2] Y. Cao, W. Yu, W. Ren, and G. Chen, "An overview of recent progress in the study of distributed multi-agent coordination," *IEEE Trans. Ind. Inform.*, vol. 9, no. 1, pp. 427–438, Feb. 2013.

[3] I. Suzuki, and M. Yamashita, "Distributed anonymous mobile robots: Formation of geometric patterns," *SIAM J. Comput.*, vol. 28, no. 4, pp. 1347–1363, 1999.

[4] K. Sugihara, and I. Suzuki, "Distributed motion coordination of multiple mobile robots," in *Proc. 5th IEEE Int. Symp. Intelligent Control*, 1990, pp. 138–143.

[5] J. A. Marshall, M. E. Broucke, and B. A. Francis, "Pursuit formations of unicycles," *Automatica*, vol. 42, no. 1, pp. 3–12, 2006.

[6] J. A. Marshall, M. E. Broucke, and B. A. Francis, "Formations of vehicles in cyclic pursuit," *IEEE Trans. Autom. Control*, vol. 49, no. 11, pp. 1963–1974, Nov. 2004.

[7] P. Lin and Y. Jia, "Distributed rotating formation control of multi-agent systems," *Syst. & Control Lett.*, vol. 59, no. 10, pp. 587–595, 2010.

[8] E. W. Justh and P. S. Krishnaprasad, "Equilibria and steering laws for planar formations," *Syst. & Control Lett.*, vol. 52, pp. 25–38, 2004.

[9] K. S. Galloway, E. W. Justh, and P. S. Krishnaprasad, "Portraits of cyclic pursuit," in *Proc. 42nd IEEE Conf. Decision and Control*, Orlando, FL, Dec. 2011, pp. 2724–2731.

[10] M. Pavone and E. Frazzoli, "Decentralized policies for geometric pattern formation and path coverage," *J. Dynam. Syst., Measur. and Control*, vol. 129, no. 5, pp. 633–643, 2007.

[11] P. Tsiotras and L. I. R. Castro, "Extended multi-agent consensus protocols for the generation of geometric patterns in the plane," in *Proc. American Control Conf.*, San Francisco, CA, Jun. 2011, pp. 3850–3855.

[12] P. Tsiotras and L. I. Reyes Castro, " The artistic geometry of consensus protocols," in *Controls and Art*. New York: Springer International, 2014, pp. 129–153.

[13] J.-C. Juang, "On the formation patterns under generalized cyclic pursuit," *IEEE Trans. Autom. Control*, vol. 58, no. 9, pp. 2401–2405, Sep. 2013.

[14] A. Morro, A. Sgorbissa, and R. Zaccaria, "Path following for unicycle robots with an arbitrary path curvature," *IEEE Trans. Robotics*, vol. 27, no. 5, pp. 1016–1023, 2011.

[15] A. Doosthoseini and C. Nielsen, "Coordinated path following for a multi-agent system of unicycles," in *Proc. 42nd IEEE Conf. Decision and Control*, Florence, Italy, Dec. 2013, pp. 2894–2899.

[16] X. Xiang, L. Lapierre, C. Liu, and B. Jouvencel, "Path tracking: Combined path following and trajectory tracking for autonomous underwater vehicles," in *Proc. Int. Conf. Intelligent Robots and Systems*, San Francisco, CA, Sep. 2011, pp. 3558–3563.

[17] T. Tripathy and A. Sinha, "Guidance of an autonomous agent for coverage applications using range only measurement," in *Proc. AIAA, Guidance, Navigation & Control Conf.*, Boston, MA, Aug. 2013. [Online]. Available: http:dx.doi.org/10.2514/6.2013-5095.

[18] T. Tripathy and A. Sinha, "A guidance law for a mobile robot for coverage applications: A limited information approach," in *Proc. 3rd Int. Conf. Advances in Control and Optimization of Dyn. Systems*, Kanpur, India, Mar. 2014, pp. 437–442.

[19] T. Tripathy and A. Sinha, "A control scheme to achieve coverage using unicycles," in *Proc. Indian Control Conf.*, Chennai, India, Jan. 2015, pp. 494–499.

[20] *The Geometry of Rene Descartes With a Facsimile of the First Edition*, New York: Dover Publications, 1954, translated by D. E. Smith and M. L. Latham.